

Coupling Capacitor Voltage Transformer: Laboratory Tests and Digital Simulations

D. Fernandes Jr., W. L. A. Neves, *Member, IEEE*, J. C. A. Vasconcelos, M. V. Godoy

Abstract-- In this work, laboratory tests of ferroresonance and circuit breaker switching were carried out for a 230 kV coupling capacitor voltage transformer (CCVT). The magnetic core and surge arrester nonlinear characteristics were taken into account in the model in order to improve the transient response to overvoltages. Digital simulations were performed using a CCVT model with linear parameters obtained from frequency response measurements. It is shown that the CCVT model is fairly accurate in reproducing ferroresonance and low frequency switching operations lab tests using digital simulations. Simulations had shown that transient overvoltages produced inside the CCVT, when a short circuit is cleared at the CCVT secondary side, are effectively damped out by the ferroresonance suppression circuit and the protection circuit. Comparisons of CCVT transient performance considering two types of surge arresters, used as protection circuits, were carried out. Voltages are damped out faster for the zinc oxide (ZnO) surge arrester as compared to silicon carbide (SiC) arrester type. Simulation of a current chopping case study is also presented.

Keywords: Coupling capacitor voltage transformer, ferroresonance, overvoltage protection, power system transients, EMTF.

I. INTRODUCTION

FOR many years, electric utilities have used coupling capacitor voltage transformers (CCVT) as input sources to protective relays and measuring instruments. The steady-state performance of the CCVT is well known. However, more investigations are necessary when these equipments are submitted to transient overvoltages, specially due to the need of laboratory measurements [1]-[3].

Brazilian electric utilities have reported unexpected overvoltage protective device operations during normal switching conditions in several 230 kV and 500 kV CCVT units, affecting the reliability of the power system and even causing failures in some CCVT units [4]. A thorough investigation of the CCVT transient behavior is needed.

In this work, ferroresonance and switching operation tests were carried out for a 230 kV CCVT unit at our high voltage laboratory in order to validate the CCVT model developed in a

The work was supported by the Brazilian National Research Council (CNPq). D. Fernandes Jr. and W. L. A. Neves are with Universidade Federal de Campina Grande (UFCG), 58.109-970, Campina Grande, PB, Brazil (e-mails: damasio@dee.ufcg.edu.br, waneves@dee.ufcg.edu.br).

J. C. A. Vasconcelos and M. V. Godoy are with Companhia Hidro Elétrica do São Francisco (CHESF), 50.761-901, Recife, PE, Brazil (e-mails: jcrabreu@chesf.gov.br, methodio@chesf.gov.br).

Presented at the International Conference on Power Systems Transients (IPST'05) in Montreal, Canada on June 19-23, 2005
Paper No. IPST05 - 076

previous work [5] in which only frequency domain measurements were available to obtain the CCVT parameters and ferroresonance digital simulations were carried out. In the present work, for validation purposes in time-domain, digital simulations were compared to lab tests of transient overvoltages, including ferroresonance tests, for the same CCVT with fairly small errors.

The obtained CCVT model was used to predict its transient response. It was observed that the ferroresonance suppression circuit and the protection circuit are very effective in damping out transient overvoltages produced inside the CCVT when a short circuit is cleared at the CCVT secondary side. Simulations of CCVT performance considering two kinds of surge arresters as protection circuit were carried out. Voltage waveforms would damp out faster if a zinc oxide (ZnO) surge arrester were used instead of the conventional silicon carbide (SiC) arrester supplied by the CCVT manufacturer.

A current chopping case study was also analyzed. This case produces one of the worst overvoltage stress to the CCVT.

II. UNDERLYING CONCEPTS

The basic electrical diagram for a typical CCVT is shown in Fig. 1. The primary side consists of two capacitive elements C_1 and C_2 connected in series. The potential transformer (PT) provides a secondary voltage v_o for protective relays and measuring instruments. The inductance L_c is chosen to avoid phase shifts between v_i and v_o at power frequency.

Ferroresonance oscillations may take place if the circuit capacitances resonate with the iron core nonlinear inductance. The oscillations cause incorrect input to relays and measuring instruments. Ferroresonance suppression circuits (FSC) tuned at power frequency (L in parallel with C) and a resistance to ground have been used to damp out oscillations requiring a small amount of energy during steady-state [3], [6]-[7].

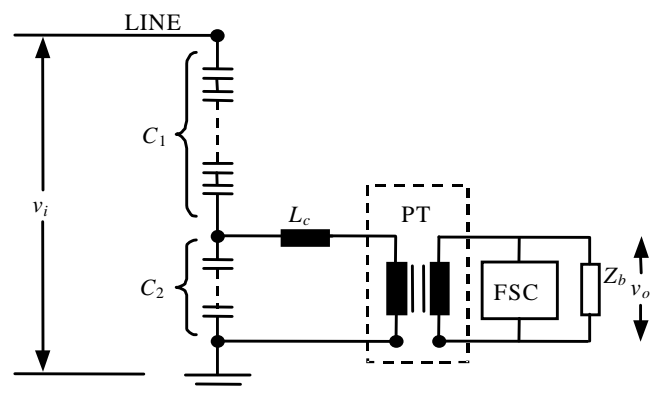


Fig. 1. Basic electrical diagram for a typical CCVT.

III. CCVT MODELING

The diagram shown in Fig. 1 is valid only near power frequency (60 Hz). A model to be applicable for frequencies in the ferroresonance range and up to a few kilohertz needs to take at least the potential transformer primary winding and compensating inductor stray capacitances effects into account [2]-[3], [6]-[7].

In this work, the circuit shown in Fig. 2 was used to model the CCVT. It comprises the following linear parameters: a capacitor stack (C_1, C_2); a compensating inductor (R_c, L_c, C_c); a potential transformer (R_p, L_p, C_p, L_m, R_m) and a ferroresonance suppression circuit ($R_f, L_{f1}, L_{f2}, -M, C_f$).

The FSC design is shown in Fig. 3(a). A nonsaturable iron core inductor L_f is connected in parallel with a capacitor C_f so that the circuit is tuned to the fundamental frequency with a high Q factor [3]. The FSC digital model is shown in Fig. 3(b). The damping resistor R_f is used to attenuate ferroresonance oscillations.

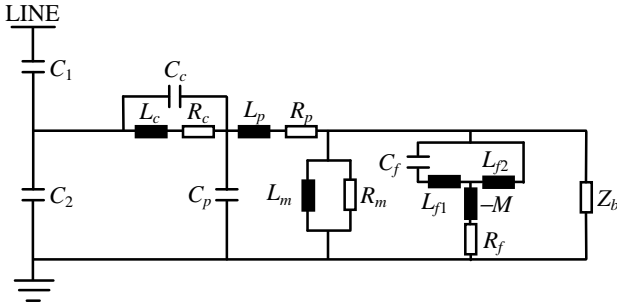


Fig. 2. CCVT model for identification of parameters.

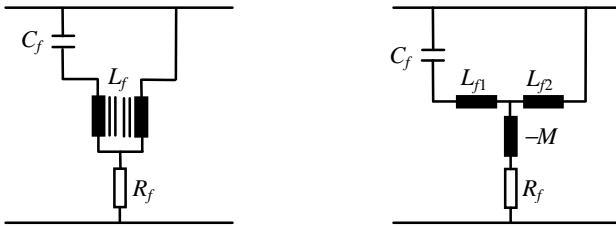


Fig. 3. (a) FSC design. (b) FSC digital model.

The circuit shown in Fig. 2 can be replaced by Fig. 4 with impedances Z_1, Z_2, Z_3, Z_4, Z_5 and all elements referred to the PT secondary side.

The expressions for the referred impedances in the s domain, with $s = j\omega$, are:

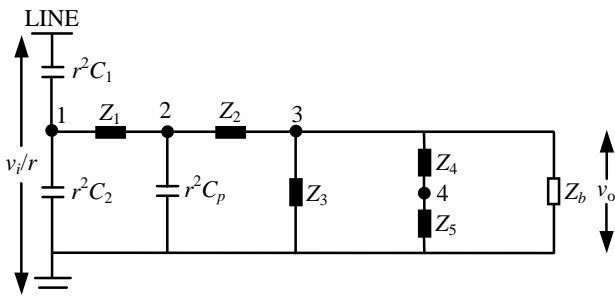


Fig. 4. CCVT model with blocks of impedances.

$$\begin{aligned} Z_1 &= \left[(R_c + sL_c) / r^2 \right] // (1 / r^2 s C_c) \\ Z_2 &= (R_p + sL_p) / r^2; \\ Z_3 &= (R_m / r^2) // (sL_m / r^2); \\ Z_4 &= (sL_{f1} + 1 / s C_f) // (sL_{f2}); \\ Z_5 &= R_f - sM. \end{aligned} \quad (1)$$

Where, r is the PT ratio and the symbol $//$ denotes that elements are in parallel. The linear parameters R, L, C were obtained from curve fitting algorithm based on Newton's method to match the transfer functions represented by the ratio v_o/v_i . This fitting technique is an improvement over the one presented in [6]-[7] because here both magnitude and phase curves are fitted simultaneously. The technique details were presented at a previous work [5].

IV. LABORATORY MEASUREMENTS

A. Frequency Response Measurements

Frequency response measurements of magnitude and phase were carried out for the 230 kV CCVT. In order to attenuate high frequency noises, a low-pass filter was connected across one of the CCVT secondary windings. A signal generator feeding an amplifier was connected across the high voltage terminal and the ground, according to Fig. 5.

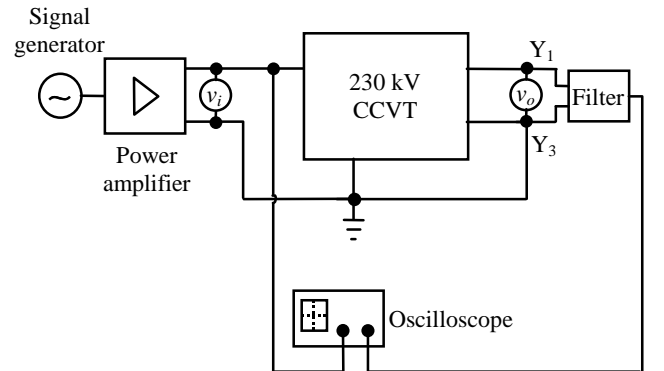


Fig. 5. Frequency response measurements for the 230 kV CCVT.

B. 230 kV CCVT Nonlinear Characteristics

The surge arrester and the magnetic core nonlinear characteristics were included in the model to give more realistic results for the simulated CCVT transient response to overvoltages. The point by point silicon carbide (SiC) surge arrester ($v - i$) curve and the PT nonlinear peak flux - current ($\lambda - i$) characteristic were estimated from laboratory measurements according to the procedures presented in [5]. The results are shown in tables I and II, respectively.

TABLE I
SILICON CARBIDE SURGE ARRESTER NONLINEAR CHARACTERISTIC.

Current (A)	Voltage (kV)
100	20.8
200	27.9
500	39.0
1000	42.9
2000	45.5

TABLE II
NONLINEAR CHARACTERISTIC OF THE PT MAGNETIC CORE.

Current (A)	Flux (V.s)
0.076368	0.025772
0.720881	0.189066
1.429369	0.396889
2.511675	0.748388
3.662012	0.863553
4.587227	0.903317
5.712037	0.942706
55.527018	1.556415
5552.7018	1.562242

V. MODEL VALIDATION

A. 230 kV CCVT Parameters from Measurements

The 230 kV CCVT constant parameters were obtained from frequency response data points of magnitude and phase measured at our high voltage laboratory. The fitted parameters are shown in Table III. The magnitude and phase curves for the measured and fitted voltage ratios are shown in figures 6 and 7, respectively.

After the fitting procedure, the average errors of magnitude and phase are, respectively, 5.2 % and 8.9° . According to figures 6 and 7, the errors are fairly small for frequencies up to 2 kHz. Near 60 Hz the magnitude and phase errors are very small. This is the region in which the CCVT operates most of the time.

TABLE III
230 kV CCVT CALCULATED PARAMETERS.

$R_c = 9.1 \text{ k}\Omega$	$L_p = 114.7 \text{ H}$	$L_{f2} = 47.39 \text{ mH}$
$L_c = 86.3 \text{ H}$	$R_m = 50.6 \Omega$	$R_f = 4.99 \Omega$
$C_c = 493.2 \text{ nF}$	$L_m = 700 \text{ mH}$	$M = 9.31 \text{ mH}$
$C_p = 9.3 \text{ pF}$	$L_{f1} = 10.87 \text{ mH}$	—
$R_p = 920 \Omega$	$C_f = 166.39 \mu\text{F}$	—

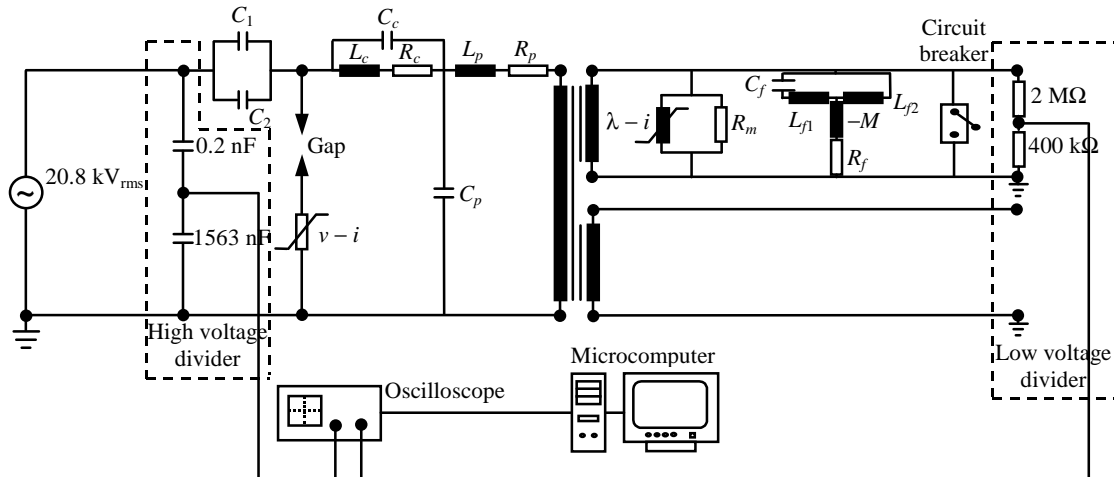


Fig. 8. Arrangement to perform the ferroresonance test for the 230 kV CCVT.

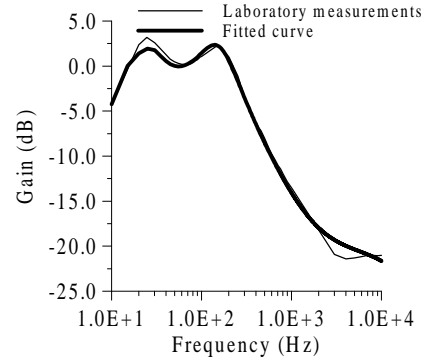


Fig. 6. Magnitude curves for the measured and fitted 230 kV CCVT voltage ratios.

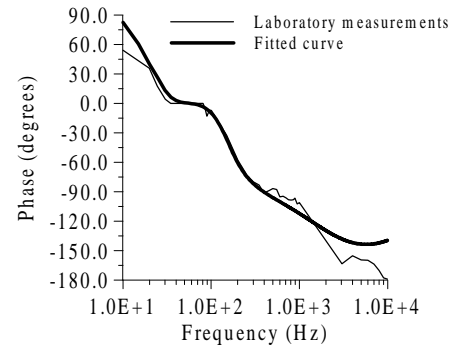


Fig. 7. Phase curves for the measured and fitted 230 kV CCVT voltage ratios.

B. Ferroresonance Test

While in the previous work [5], only ferroresonance simulations were performed to analyze the CCVT transient behavior, in this work the ferroresonance test was carried out in order to validate the CCVT model in time-domain studies. IEC 186 Standard [8] establishes that for the ferroresonance test the CCVT must be energized at 1.2 per unit of rated voltage. One of the CCVT secondary terminals with a nearly zero burden is then short-circuited. The short-circuit must be sustained during three cycles, at least.

For electromagnetic transient studies, the CCVT model is shown in Fig. 8.

The silicon carbide surge arrester (original arrester which is part of the CCVT unit) was included in the model. Its $v - i$ nonlinear characteristic is shown in Table I. The PT magnetizing branch is represented by a nonlinear inductance connected across the CCVT secondary terminals whose $\lambda - i$ data points are shown in Table II.

In order to perform the ferroresonance test in laboratory, a 20.8 kV rms voltage source was used and the CCVT capacitors C_1 and C_2 were connected in parallel, according to the Fig. 8. The short-circuit at the CCVT secondary winding was performed using a 17.5 kV, 630 A circuit breaker.

The voltage signals across the two voltage dividers were recorded using a digital oscilloscope and the data saved in a microcomputer. The recorded voltage obtained from the high voltage divider was used as the input voltage source to obtain the digital simulations for the voltage at the CCVT secondary terminals. Fig. 9 shows the measured and simulated CCVT secondary voltage waveforms. The full line represents the results obtained from the laboratory measurements and the dotted line represents the results obtained from the CCVT model.

The digital simulations were performed using the ATP (Alternative Transients Program) [9]. The short-circuit was initiated at $t = 102$ ms and sustained during 55 ms, approximately.

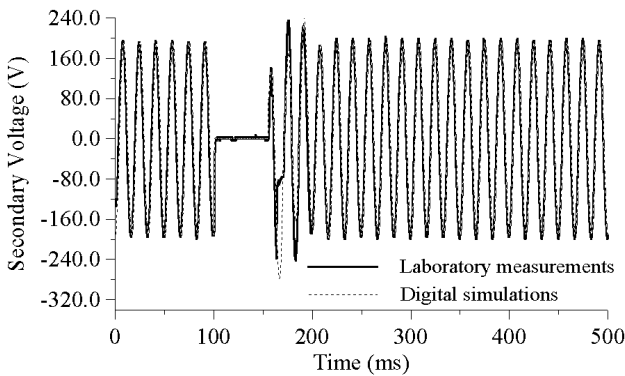


Fig. 9. Measured and simulated CCVT secondary voltage waveforms when the CCVT is submitted to the ferroresonance test.

There is good agreement between lab tests and simulations except for the second positive and negative peaks of voltage waveforms. This may be because the breaker was modeled as an ideal switch, neglecting the effect of the arc in the breaker.

C. Circuit Breaker Switching at the CCVT Primary Side

Another test performed to validate the CCVT model was the measurement of the CCVT secondary voltage due to switching operations. The breaker was moved to the position shown in Fig. 10 and a sinusoidal voltage waveform of 17.4 kV rms was used. The transient response was measured during the close-open switch operation. Again, the recorded voltage obtained from the high voltage divider was used as the input voltage source to obtain the digital simulations for the voltage at the CCVT secondary terminals. The dividers here have different voltage ratios from the ones used in the ferroresonance test because voltages are more severe for the ferroresonance case and might damage the oscilloscope.

Fig. 11 shows the CCVT voltage waveform at the CCVT secondary side when the circuit breaker is switched on. The solid line represents the results obtained from laboratory and the dotted line represents the results obtained from digital simulations. The breaker contact closes at $t = 24$ ms and remains closed during approximately 60 ms. The voltage waveforms obtained from laboratory measurements and from digital simulations show good agreement.

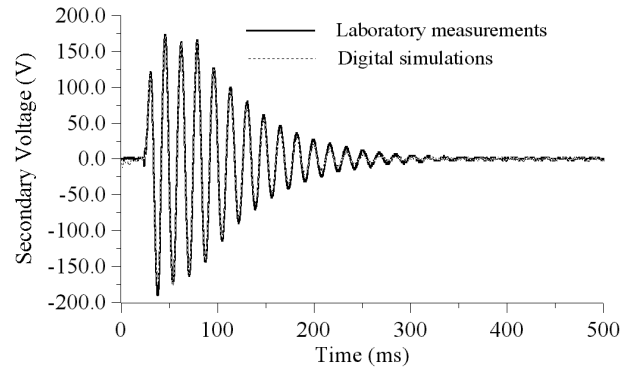


Fig. 11. Measured and simulated CCVT secondary voltage waveforms during switching operations at the CCVT primary side.

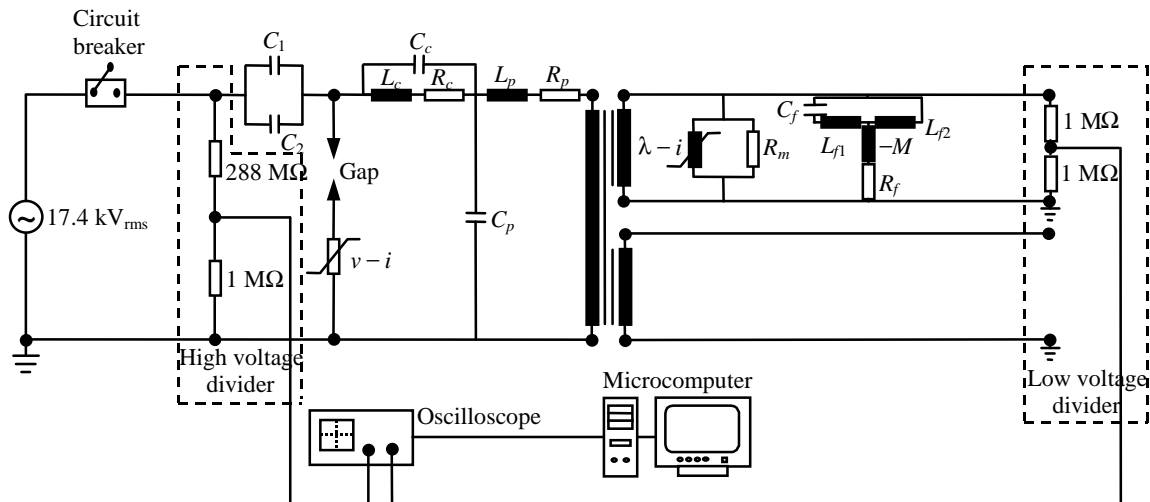


Fig. 10. Arrangement to perform the circuit breaker switching at the 230 kV CCVT primary side.

VI. SIMULATION RESULTS

With the CCVT model validated in time and frequency domains, some digital simulations were performed to predict the CCVT behavior under transient overvoltages.

A. Ferroresonance Simulations

The importance of the FSC in damping out transients produced inside the CCVT was analyzed by performing two ferroresonance simulations: the first one with the FSC included in the CCVT model and the second one ignoring the FSC. In both cases, the simulations consist of a close-open operation of the switch connected across the CCVT secondary terminals, as shown in Fig. 8. The switch closes at $t = 125$ ms and remains closed during 6 cycles, when the short-circuit is cleared [10].

The absolute value of the inductance M used in simulations was equal to 8.84 mH instead of the 9.31 mH value shown in Table III to ensure numerical stability of the FSC model for all frequencies, although this does not affect the CCVT frequency response in the ferroresonance region [5], [10].

Fig. 12 shows the CCVT secondary voltage waveform when the FSC is ignored. The oscillations remain up to 500 ms, when the steady-state is reached. Fig. 13 shows the same case with the FSC included in the CCVT model. The oscillations are damped in a time smaller than 100 ms, in conformity to ferroresonance standard tests.

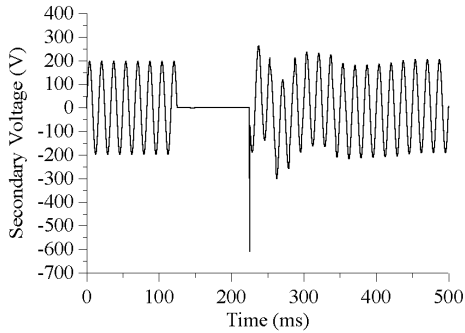


Fig. 12. Transient secondary voltage: CCVT without FSC.

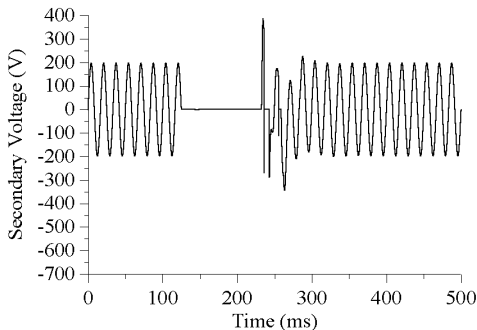


Fig. 13. Transient secondary voltage: CCVT with FSC.

B. Simulations of the CCVT Protection Circuit

The performance of the CCVT protection circuit was addressed through digital simulations. The CCVT silicon carbide (SiC) surge arrester performance was compared to the one of a zinc oxide (ZnO) surge arrester with the same rated voltage, whose $v - i$ characteristic was estimated from [11].

Fig. 14 shows the comparisons between CCVT secondary voltages when the protection circuit is composed by SiC surge arrester (dotted line) and ZnO surge arrester (solid line). The performance for both arresters are very similar, however the voltage is damped out faster with the ZnO surge arrester. In Fig. 15 the effect of the surge arrester is ignored. From Fig. 15 and Fig. 14, one can see that the protection circuit is very effective in limiting overvoltages produced inside the CCVT, when a short-circuit is cleared at the CCVT secondary side.

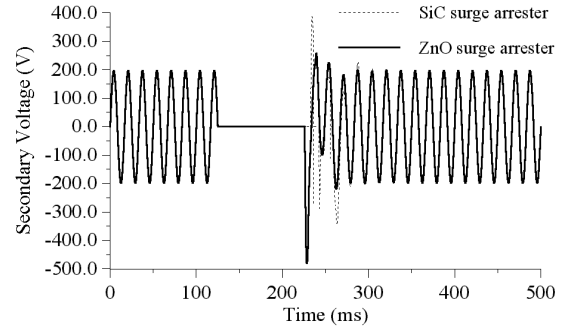


Fig. 14. Transient CCVT secondary voltages: comparisons between protection circuit composed by SiC and ZnO surge arresters.

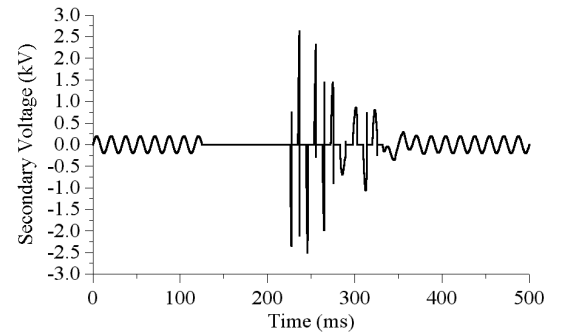


Fig. 15. Transient CCVT secondary voltage: surge arrester effects are ignored.

C. Current Chopping Simulations

Fig. 16 shows a typical power system configuration in which the CCVT is disconnected from the 230 kV opening the switch SW when the current is different from zero value. All breakers D are closed. Fig. 17 shows the CCVT secondary voltage for current chopping when the FSC is included in the model (solid line) and ignored (dotted line). The current chopping produces a severe overvoltage with high frequency at the CCVT secondary side. The high voltage is due to the increase of the voltage across the inductive elements when the current is abruptly cut. The FSC is very important in damping out CCVT transient voltages.

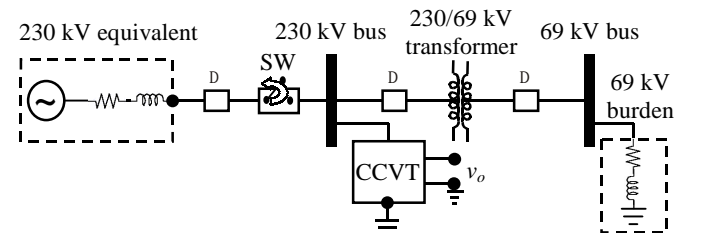


Fig. 16. Typical power system configuration for current chopping simulations near the CCVT primary side.

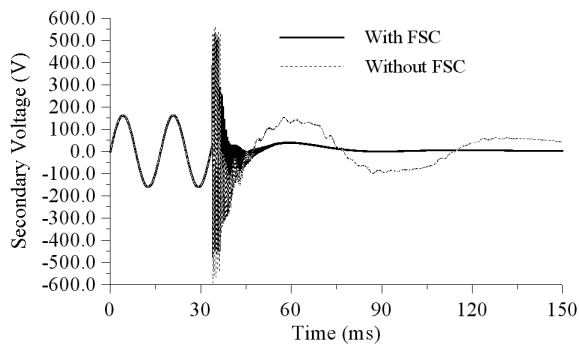


Fig. 17. Transient secondary voltage for current chopping: CCVT with and without FSC.

VII. CONCLUSIONS

In this work, laboratory tests of ferroresonance and circuit breaker switching were carried out for a 230 kV CCVT unit. The used CCVT model was validated from frequency response measurements, in the range from 10 Hz to 10 kHz, for both magnitude and phase of the CCVT transfer functions. The magnetic core and surge arrester nonlinear characteristics were taken into account in the model in order to improve the transient response to overvoltages.

The validation of model in time-domain was achieved when simulations and measurements were compared against and shown that the CCVT model is fairly accurate.

There was a good agreement between laboratory tests and digital simulations for ferroresonance and circuit breaker switching operations. Because of this the model was used in connection with the ATP to predict the CCVT performance when it is submitted to transient overvoltages.

Simulation results had shown how important are the ferroresonance suppression circuit and the protection circuit in damping out and limiting transient voltages produced inside the CCVT, when a short circuit is cleared at the CCVT secondary side. It was also seen that voltages were damped out faster with the zinc oxide (ZnO) surge arrester compared with the silicon carbide (SiC) surge arrester when they are used as CCVT protection circuit.

The current chopping simulation results shown that the phenomenon produces one of the worst overvoltage stress for the CCVT because a severe voltage with high frequency takes place at the CCVT secondary side.

VIII. ACKNOWLEDGMENTS

The authors wish to thank the CHESF for providing a 230 kV CCVT unit. The authors are also very grateful to the reviewers for their invaluable suggestions.

IX. REFERENCES

- [1] J. R. Lucas, P. G. McLaren, W. W. L. Keerthipala, and R. P. Jayasinghe, "Improved Simulation Models for Current and Voltage Transformers in Relay Studies," *IEEE Trans. Power Delivery*, vol. 7, no. 1, pp. 152-159, Jan. 1992.
- [2] M. R. Iravani, X. Wang, I. Polishchuk, J. Ribeiro, and A. Sarshar, "Digital Time-Domain Investigation of Transient Behaviour of Coupling

- Capacitor Voltage Transformer," *IEEE Trans. Power Delivery*, vol. 13, no. 2, pp. 622-629, Apr. 1998.
- [3] D. A. Tziouvaras, P. McLaren, G. Alexander, D. Dawson, J. Ezstergalyos, C. Fromen, M. Glinkowski, I. Hasenwinkle, M. Kezunovic, Lj. Kojovic, B. Kotheimer, R. Kuffel, J. Nordstrom, and S. Zocholl, "Mathematical Models for Current, Voltage and Coupling Capacitor Voltage Transformers," *IEEE Trans. Power Delivery*, vol. 15, no. 1, pp. 62-72, Jan. 2000.
- [4] H. M. Moraes and J. C. A. Vasconcelos, "Overvoltages in CCVT During Switching Operations," (In Portuguese), in *Proc. 1999 National Seminar on Production and Transmission of Electrical Energy*, Foz do Iguaçu, Brazil.
- [5] D. Fernandes Jr., W. L. A. Neves, and J. C. A. Vasconcelos, "A Coupling Capacitor Voltage Transformer Representation for Electromagnetic Transient Studies," in *Proc. 2003 International Conference on Power Systems Transients*, New Orleans, USA.
- [6] M. Kezunovic, Lj. Kojovic, V. Skendzic, C. W. Fromen, D. R. Sevcik, and S. L. Nilsson, "Digital Models of Coupling Capacitor Voltage Transformers for Protective Relay Transient Studies," *IEEE Trans. Power Delivery*, vol. 7, no. 4, pp. 1927-1935, Oct. 1992.
- [7] Lj. Kojovic, M. Kezunovic, V. Skendzic, C. W. Fromen, and D. R. Sevcik, "A New Method for the CCVT Performance Analysis Using Field Measurements, Signal Processing and EMTP Modeling," *IEEE Trans. Power Delivery*, vol. 9, no. 4, pp. 1907-1915, Oct. 1994.
- [8] *Voltage Transformers*, IEC 186, First Supplement (1970), Amendment no. 1, 1978.
- [9] Leuven EMTP Center, *ATP - Alternative Transients Program - Rule Book*, Heverlee, Belgium, Jul. 1987.
- [10] D. Fernandes Jr., "Coupling Capacitor Voltage Transformers Model for Electromagnetic Transient Studies," (In Portuguese), D.Sc. thesis, Dept. Electrical Engineering, Federal University of Campina Grande, Campina Grande, 2003.
- [11] E. G. Costa, "Analysis of Zinc Oxide Surge Arrester Performance," (In Portuguese), D.Sc. thesis, Dept. Electrical Engineering, Federal University of Paraíba, Campina Grande, 1999.

X. BIOGRAPHIES

Damásio Fernandes Jr. was born in Brazil in 1973. He received the B.Sc. and M.Sc. degrees in electrical engineering from Universidade Federal da Paraíba (UFPB) in 1997 and 1999, respectively, and the D.Sc. degree in electrical engineering from Universidade Federal de Campina Grande (UFCG) in 2004. Since 2003, he is with the Department of Electrical Engineering of UFCG, Campina Grande, PB, Brazil. His research interests are electromagnetic transients and optimization for power system applications.

Washington L. A. Neves (SM'1991, M'1995) was born in Brazil in 1957. He received the B.Sc. and M.Sc. degrees in electrical engineering from Universidade Federal da Paraíba (UFPB) in 1979 and 1982, respectively, and the Ph.D. degree from the University of British Columbia, Vancouver, Canada, in 1995. From 1982 to 1985 he was with the Department of Electrical Engineering of Faculdade de Engenharia de Joinville, Brazil. From 1985 to 2002 he was with the Department of Electrical Engineering of UFPB, Campina Grande, PB, Brazil. Since 2002, he is with the Department of Electrical Engineering of Universidade Federal de Campina Grande (UFCG), Campina Grande, PB, Brazil.

José Carlos A. Vasconcelos was born in Brazil in 1952. He received the B.Sc. degree in electrical engineering from Universidade Federal de Pernambuco (UFPE) in 1976 and the M.Sc. degree in electrical engineering from Universidade Federal da Paraíba (UFPB) in 2001. He is currently with the Companhia Hidro Elétrica do São Francisco (CHESF), Recife, PE, Brazil.

Methodio V. Godoy was born in Brazil in 1959. He received the B.Sc. degree in electrical engineering from Universidade Federal de Pernambuco (UFPE) in 1982, the M.Sc. degree in electrical engineering from UMIST, Manchester, England in 1995, and he is currently D.Sc. student at UFPE. He is with the Companhia Hidro Elétrica do São Francisco (CHESF) and he is a lecturer of the Department of Electrical Engineering of Universidade de Pernambuco (UPE), Recife, PE, Brazil.